Effects of Random Phase and Amplitude Errors in Optical Fiber Bragg Gratings

Ricardo Feced and Michalis N. Zervas

Abstract—This paper studies the influence of random phase and amplitude fabrication errors on the performance of optical filters based on fiber Bragg gratings (FBG's). In particular, we analyze two effects of particular importance for optical communications: the excess crosstalk induced in apodized gratings commonly used in wavelength-division-multiplexing (WDM) systems, and the time-delay fluctuations that appear in chirped gratings employed to compensate the fiber dispersion. A statistical model is presented to explain these effects in terms of the coherence length of the grating fabrication procedure.

Index Terms—Gratings, noise, optical fiber communication.

I. INTRODUCTION

THE performance of optical components is usually degraded by random fluctuations of their optical or geometrical properties. Rayleigh scattering, for instance, is a typical example of scattering induced by random fluctuations of an optical property of the medium: the refractive index [1], [2]. On the other hand, random deviations of the device geometry, like roughness of its surfaces or randomness in the periodicity of gratings, can also be responsible for enhanced scattering in many optical components [3]. In this paper, we investigate the effect of random optical and geometrical fluctuations on the performance of optical fiber gratings (OFG's) as optical filters.

The problem of random propagation in one dimension has been extensively studied in many different contexts [4]–[6]. The moment-propagation method, for example, studies the evolution of the second order field statistics along the medium, and can be used to predict the amount of backscattered power [4], [5]. Sometimes, it is important to analyze not only the scattered power, but also the evolution of the optical phase of the propagating wave. This is specially important for interferometric optical devices, where fluctuations of the waveguide effective refractive index can give rise to a random-walk of the optical phase that deteriorates their performance [7], [8].

In recent years, OFG's have become key components in high speed optical fiber communication systems. The technology of UV photoinduced fiber gratings [9] has reached now high maturity, enabling the fabrication of complex OFG-based filters to perform various functions such as selection of wavelength multiplexed channels or compensation of the link dispersion. Several experimental techniques have been demonstrated to fabricate nonuniform gratings, permitting an accurate control of both the local grating period and the apodization profile along the

structure [10], [11]. However, the fabrication of increasingly longer OFG's with improved spectral response is limited by the need to maintain the coherence of the grating phase along the whole structure. Numerical experiments have shown that random coupling can have important implications in the performance of practical filters [3], [12].

In this paper, we study the effect of small random phase or amplitude fluctuations imprinted on the grating during the fabrication process on the spectral response of the filter. We will present a method to calculate the main statistics of the filter response, like average reflectivity or average time-delay fluctuations, in terms of a characteristic coherence length of the grating. The method, which relies on a perturbation approach, calculates ensemble averages of the spectral response parameters of gratings perturbed with a random-walk phase. In particular, we will focus on two cases of particular importance for optical communications: the excess crosstalk induced in apodized gratings commonly used in wavelength-division-multiplexing (WDM) systems, and the time-delay fluctuations that appear in chirped gratings employed to compensate the fiber dispersion. The paper is organized as follows. Section II describes the propagation in OFG's subjected to random phase and amplitude errors. The statistical averages for the main parameters of their spectral response is then calculated in Section III. We finally apply the theory developed to the two particular cases previously discussed: apodized (Section IV), and chirped (Section V) OFG's.

II. PROPAGATION IN FIBER GRATINGS WITH RANDOM PHASE AND AMPLITUDE EVOLUTION

In this section, we describe the optical propagation in OFG's with random phase or amplitude errors along their structure. The magnitude of the phase errors will be characterized in terms of a "coherence length" for the grating. In the following sections, we will present a method to calculate ensemble averages of the main parameters of the OFG spectral response, and discuss their dependence on the coherence length previously introduced.

A. Refractive Index Perturbation in Fiber Gratings

Bragg gratings are fabricated in optical fibers by exposing their core to a periodic ultraviolet (UV) pattern. Initially, a holographic method based on an split-beam interferometer [9] demonstrated the possibility of writing gratings by means of transverse UV exposure. A more recent development, that greatly simplifies the requirements of the OFG fabrication setup, is the use of diffractive optical phase-mask gratings [13], [14]. A third technique in which the grating is transversely

written point by point by accurately controlling the position and spot size of the UV beam has also been demonstrated [15]. These three basic techniques have been modified and improved to fabricate long gratings with accurate control over the photo-induced refractive index modulation. The first extension is the phase-mask scanning technique in which the laser beam is scanned over a long and high-quality phase-mask [10], [16]. An alternative procedure to write long gratings is to accurately move and monitor the position of the fiber by means of an interferometer while exposing it to a time-modulated short UV interference pattern [11]. This is probably the most versatile approach, and complex filters designs have been demonstrated with this technique [17], [18].

Independently of the technique used to write OFG, phase and amplitude errors are likely to occur due to the stringent requirements of accuracy and stability necessary in the fabrication process. There are a great variety of possible sources for these errors. Some of them are associated with the fabrication method, like phase-errors of phase masks, uncertainty of the fiber position in interferometrically controlled methods, lack of mechanical stability of the fabrication setup, or fluctuations in the UV fluence. Others are intrinsic to the photosensitive fiber, like geometrical or compositional fluctuations.

The effective refractive index $n(z)$ along an OFG can be described as

$$n(z) = n_o + \left\{ \frac{\Delta n(z)}{2} e^{j[K_o z + \theta(z) + \phi(z)]} (1 + F_a(z)) + \text{c.c.} \right\} \tag{1}$$

where n_o is the average effective refractive index, and $K_o(= 2\pi/\Lambda)$, $\Delta n(z)$ and $\theta(z)$ specify the deterministic grating parameters: Λ is a reference period, $\Delta n(z)$ accounts for the local grating strength (apodization), and $\theta(z)$ will determine its phase variation and local period. The random properties of the grating are described by the phase and amplitude stochastic processes $\phi(z)$ and $F_a(z)$. The local period $\Lambda(z)$ of the grating is determined by both the deterministic phase term $\theta(z)$ and the random phase term $\phi(z)(\Lambda^{-1}(z) = \Lambda^{-1} + (\theta' + \phi')/2\pi$.

The phase and the amplitude noise are usually partially correlated. Fluctuations of the fluence during the fabrication process contribute to both sources of noise, giving rise to some correlation among them. However, in this paper we study the effects of the phase and amplitude noises separately, as if they were statistically independent. The method presented could easily be extended to take into account phase-amplitude correlations.

1) Phase-Noise: We will assume that the random fluctuations of the local spatial angular frequency $(=2\pi/\Lambda(z))$ along the grating can be modeled by a zero-average, stationary, Gaussian process $F_\phi(z)$. Fig. 1 illustrates the evolution of the refractive index perturbation in a grating subjected to random phase-noise. The phase term $\phi(z)$ in (1) will be driven by $F_\phi(z)$ according to the expression

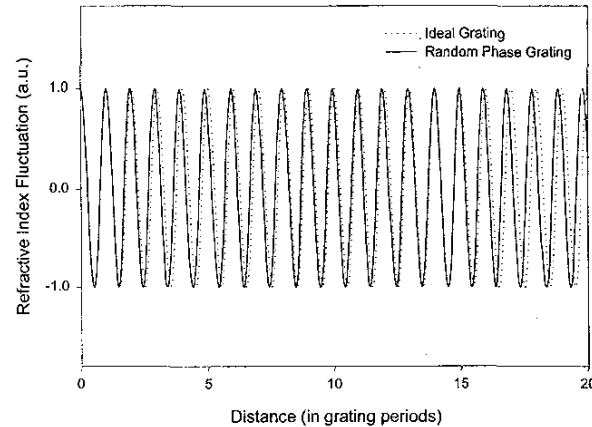$$\phi(z + \Delta) - \phi(z) = \int_z^{z+\Delta} d\tau \ F_\phi(\tau). \tag{2}$$

Fig. 1. Illustration of a grating subjected to phase errors. - - - :Ideal grating. —— :Grating with phase-noise.

The variance for the increments of $\phi(z)$ can now be calculated as [19]

$$\sigma^2(\phi(z + \Delta) - \phi(z)) = \int_{-\Delta}^{\Delta} d\tau(\Delta - |\tau|) \ R_{F\phi}(\tau) \tag{3}$$

where $R_{F\phi}(\tau)$ is the autocorrelation function for $F_\phi(z)$. In standard OFG fabrication techniques the correlation length for $F_\phi(z)$ is usually much smaller than the grating length and, therefore, its spectrum is broad compared to the grating spectral response. Consequently, in most situations we can regard $F_\phi(z)$ as a white Gaussian noise. In this case, the phase $\phi(z)$ evolves as a Brownian random-walk motion [19], [20], being driven by the delta-correlated Langevin force $F_\phi(z)$ that accounts for random fluctuations of the local period along the grating. $\phi(z)$ will also follow Gaussian statistics, with independent increments, and zero average. In analogy with a single-mode laser, we will define both a "coherence length" L_{coh} and a "linewidth parameter" γ that characterizes the variance σ^2 of the increments of $\phi(z)$ [21]

$$\sigma^2(\phi(z + \Delta) - \phi(z)) = \frac{2}{L_{coh}}|\Delta| = 4\gamma|\Delta| \tag{4}$$

where $R_{F\phi}(\tau)$ was taken equal to $2\delta(\tau)/L_{coh}$ in (3), $\delta(\tau)$ being the Dirac delta. From (4), we see that the standard deviation of the random phase variation along a grating period Λ is $\sqrt{2\Lambda/L_{coh}}$. The Gaussian nature of the increments of $\phi(z)$ permits the calculation of the autocorrelation $\Re(\Delta)$ of the random phase term in (1)

$$\Re(\Delta) = \left\langle e^{j(\phi(z+\Delta)-\phi(z))} \right\rangle$$
$$= e^{-\sigma^2/2} = e^{-|\Delta|/L_{coh}} = e^{-2\gamma|\Delta|} \tag{5}$$

where $\langle \cdot \rangle$ stands for ensemble average. The "coherence length" L_{coh} previously defined measures the distance along which there is substantial dephasing with respect to the perfect deterministic grating. It can be regarded as a figure of merit for the grating fabrication system, being ideally as large as possible.

2) Amplitude Noise: Following the same reasoning as in the previous section, we will assume that the amplitude noise

process $F_a(z)$ in (1) is a zero-average, Gaussian white-noise. Consequently, its autocorrelation will be

$$\langle F_a(z+\tau)F_a(z)\rangle = \eta\delta(\tau) \tag{6}$$

where the factor η provides a measure for the magnitude of the amplitude noise. If the grating is sampled in small sections of length Δ, then the variance of the relative amplitude fluctuations for each sample is given in terms of η by

$$\sigma_a^2 = \frac{\eta}{\Delta} \tag{7}$$

Δ can be considered as the inverse of a maximum cutoff spatial frequency for the white noise. Its value is primarily determined by the writing method and is usually of the order of a few hundred microns. As typical noise cutoff frequencies correspond to optical reflection bandwidths much broader than those of the deterministic OFG's, the assumption of delta-correlated noise sources is expected to be a good approximation in most physical situations. However, the method presented in following sections to calculate ensemble averages does not rely on this assumption, and can be generalized to take into account different statistics for the noise sources.

B. Coupled-Mode Equations

The one-dimensional scattering problem for an OFG is usually described in the framework of the coupled-mode formalism [22]–[24]. The scattering equations are written in terms of two counter-propagating waves, $b_B(z, \beta)$, backward propagating, and $b_F(z, \beta)$, forward propagating

$$\frac{db_B(z, \beta)}{dz} - j\beta b_B(z, \beta) = -q(z)b_F(z, \beta)$$
$$\frac{db_F(z, \beta)}{dz} + j\beta b_F(z, \beta) = -q^*(z)b_B(z, \beta) \tag{8}$$

where β is the detuning parameter

$$\beta = \frac{2kn_o - K_o}{2} \tag{9}$$

and k is the vacuum propagation constant ($=\omega/c$). $q(z)$ is related to the grating parameters as

$$q(z) = \frac{jK_o}{2n_o}\frac{\Delta n(z)}{2}e^{j(\theta(z)+\phi(z))}(1 + F_a(z))$$
$$= q_o(z)e^{j\phi(z)}(1 + F_a(z)) \tag{10}$$

where $q_o(z)$ is the deterministic part of the coupling function.

The OFG reflection spectral response $H_R(\beta)$ can be calculated by solving (8) taking into account the appropriate boundary conditions, i.e., $b_F(0, \beta) = 1$ and $b_B(L, \beta) = 0$, where L is the total length of the grating

$$H_R(\beta) = b_B(0, \beta). \tag{11}$$

The actual backward and forward electric fields ($e_B(z, \beta)$ and $e_F(z, \beta)$) are related to the waves $b_B(z, \beta)$ and $b_F(z, \beta)$ through the expressions

$$e_B(z, \beta) = b_B(z, \beta)e^{+j(K_o z/2)}$$
$$e_F(z, \beta) = b_F(z, \beta)e^{-j(K_o z/2)}. \tag{12}$$

The main novelty of the present study is that the coupling function $q(z)$ is an stochastic process characterized by the coherence length L_{coh} of the fabrication system. We could calculate ensemble averages for the main parameters of the OFG spectral response by repetitive solution of the coupled-mode equations (8) for different realizations of the stochastic process $\phi(z)$, and subsequent average of the parameters of interest. This would yield information about the average behavior of a batch of gratings written with that fabrication system. In this paper we develop an alternative method to calculate directly these ensemble averages without the need of statistical averages over many realizations of the experiment. The study illustrates the effects of phase and amplitude errors in the performance of OFG and provides insight in the interrelations among the various grating and fabrication system parameters.

C. Approximate Spectral Response for OFG Perturbed with Random Noise

The main difficulty to calculate ensemble averages for parameters related with the OFG spectral response $H_R(\beta)$ is the nonlinear relation existing between $H_R(\beta)$ and the coupling function $q(z)$. Simple linear approximations like the first-order Born approximation are inaccurate for the analysis of practical gratings with reflectivities larger than 50%. In this section we will present a novel linearization method that will enable us to calculate ensemble averages in gratings with random phase and amplitude errors. The method relies on a perturbational analysis with respect to the solution of the ideal deterministic grating characterized by $q_o(z)$ given in (10).

Our objective is to express the reflection coefficient $H_R(\beta)$ (11) as a linear function of the stochastic coupling function $q(z)$ with a good degree of accuracy. The procedure starts by solving exactly the coupled-mode equations for the corresponding deterministic case characterized by the coupling function $q_o(z)$. The solution of the deterministic equation yields the evolution of the forward and backward deterministic propagation waves $b_F^o(z, \beta)$ and $b_B^o(z, \beta)$, and also the spectral response of the unperturbed grating $H_R^o(\beta)$. An approximate expression for the spectral response of the perturbed grating $H_R(\beta)$ can now be obtained by substituting the calculated forward deterministic wave $b_F^o(z, \beta)$ for $b_F(z, \beta)$ in the first equation of system (8), and integrating then the resulting ordinary linear differential equation. The spectral response can be cast in an expression that looks very similar to the first-order Born approximation with a modified coupling function $\tilde{q}(z, \beta)$

$$H_R(\beta) = \int_{z=0}^{L} dz\, \tilde{q}(z, \beta)e^{-2j\beta z} \tag{13}$$

where the modified coupling function $\tilde{q}(z, \beta)$

$$\tilde{q}(z, \beta) = \tilde{q}_o(z, \beta)e^{j\phi(z)}(1 + F_a(z)) \tag{14a}$$

$$\tilde{q}_o(z, \beta) \equiv q_o(z)\left[b_F^o(z, \beta)e^{j\beta z}\right]. \tag{14b}$$

Equation (14b) defines the deterministic modified coupling function $\tilde{q}_o(z, \beta)$. This modified coupling function can be approximated by $q_o(z)$ in those parts of the β-spectrum where the

grating reflectivity is low. The spectral response $H_R(\beta)$ is now a stochastic process obtained from a linear transformation of the random coupling function $q(z)$.

The OFG spectral response given in (13) is obviously exact in the deterministic case, i.e., when phase and amplitude errors are negligible. If the grating has a long coherence length L_{coh} and a low amplitude-noise factor η, then the random terms in (14) can be regarded as a small perturbation and (13) gives a good approximation to the grating spectral response. The accuracy of this analysis will be corroborated in following sections by Monte Carlo-type simulations in which the spectral response of a batch of randomly generated gratings will be averaged to obtain estimations for ensemble averages.

III. ENSEMBLE AVERAGES FOR GRATING REFLECTIVITY AND TIME DELAY FLUCTUATIONS

The two parameters that fully characterize the spectral response of OFG are its reflectivity and time-delay response. They are, respectively, related to the modulus $|H_R(\beta)|$ and phase $\varphi_R(\beta)$ of the spectral response $H_R(\beta)$. In this section we will derive expressions to calculate ensemble averages for these parameters in presence of both phase-noise (Sections III-A–III-C) and amplitude-noise (Section III-D) in the grating coupling function.

A. Ensemble Averages for Random Phase Functions

Let us assume first that the grating is only subjected to random phase errors, i.e., $F_a(z) = 0$. All the phase-noise ensemble averages that we will need are particular cases of the ensemble average of a general stochastic process $F(\beta; \tilde{g}(z, \beta), \tilde{h}(z, \beta))$ defined as

$$
F\left(\beta;\; \tilde{g}(z, \beta),\; \tilde{h}(z, \beta)\right)
= \int_0^L dy \int_0^L dx\; \tilde{g}(y, \beta)\, \tilde{h}^*(x, \beta)\, e^{-2j\beta(y-x)} \tag{15}
$$

where * stands for complex conjugate, and $\tilde{g}(z, \beta)$ and $\tilde{h}(z, \beta)$ are random phase functions defined as the product of the deterministic functions $\tilde{g}_o(z, \beta)$ and $\tilde{h}_o(z, \beta)$, and the random phase term $e^{j\phi(z)}$, namely

$$
\begin{aligned}
\tilde{g}(z, \beta) &= \tilde{g}_o(z, \beta)e^{j\phi(z)} \\
\tilde{h}(z, \beta) &= \tilde{h}_o(z, \beta)e^{j\phi(z)}.
\end{aligned} \tag{16}
$$

To calculate the ensemble average $\langle F(\beta;\; \tilde{g}(z, \beta),\; \tilde{h}(z, \beta))\rangle$ we first substitute (16) in (15) and, subsequently, evaluate the ensemble average for the random phase terms with the autocorrelation (5). Finally, by transforming the independent variables

$$
\begin{aligned}
\tau &= y - x \\
z &= x
\end{aligned} \tag{17}
$$

we obtain the following expression for the sought average $\overline{F}(\beta;\; \tilde{g}_o(z, \beta),\; \tilde{h}_o(z, \beta);\; \gamma)$:

$$
\begin{aligned}
&\overline{F}\left(\beta;\; \tilde{g}_o(z, \beta),\; \tilde{h}_o(z, \beta);\; \gamma\right) \\
&= \left\langle F\left(\beta;\; \tilde{g}(z, \beta),\; \tilde{h}(z, \beta)\right)\right\rangle \\
&= \int_{-L}^L d\tau \int_{-\infty}^{\infty} dz\; \tilde{g}_o(z + \tau, \beta)\, \tilde{h}_o^*(z, \beta)\, e^{-2\gamma|\tau|}\, e^{-2j\beta\tau}
\end{aligned} \tag{18}
$$

where we see that it involves a cross-correlation integral followed by a weighted Fourier transform.

B. Average for the Reflectivity in OFG with Phase-Noise

The ensemble average for the reflectivity can be calculated from the approximate spectral response $H_R(\beta)$ described in (13) together with the method for evaluation of ensemble averages shown in (18). Defining the ensemble average for the reflectivity as $\langle R(\beta)\rangle$, we find

$$
\begin{aligned}
\langle R(\beta)\rangle &= \langle H_R(\beta)H_R^*(\beta)\rangle \\
&= \left\langle \int_0^L dy \int_0^L dx\; \tilde{q}(y, \beta)\tilde{q}^*(x, \beta)e^{-2j\beta(y-x)}\right\rangle \\
&= \overline{F}(\beta; \tilde{q}_o(z, \beta), \tilde{q}_o(z, \beta); \gamma)
\end{aligned} \tag{19}
$$

which is calculated as the autocorrelation of $\tilde{q}_o(z, \beta)$ followed by a Fourier transform weighted by a decaying exponential (18).

C. Averages for the Time Delay and its fluctuations in OFG with Phase-Noise

The estimation of the average time-delay and its fluctuations is of particular importance for phase-filters like OFG dispersion compensators. Generally, the quality of OFG dispersion compensators is evaluated through the standard deviation of its time-delay [25]. For this type of filters, the phase of the spectral response $\varphi_R(\beta)$ varies rapidly within the reflection band in comparison with its modulus $|H_R(\beta)|$. This fact will permit us to estimate ensemble averages for the time delay of OFG dispersion compensators.

1) Average Time Delay: The time-delay $t_d(\beta)$ is defined in terms of the spectral phase response $\varphi_R(\beta)$ as

$$
t_d(\beta) = -\frac{n_o}{c}\frac{\partial\varphi_R(\beta)}{\partial\beta}. \tag{20}
$$

In the presence of random phase errors, $t_d(\beta)$ is a stochastic process. To estimate the ensemble average for the time-delay $\langle t_d(\beta)\rangle$, we start with the related ensemble average

$$
\begin{aligned}
&\left\langle \frac{\partial H_R(\beta)}{\partial\beta}H_R^*(\beta)\right\rangle \\
&= \left\langle |H_R(\beta)|\frac{\partial|H_R(\beta)|}{\partial\beta} + j\frac{\partial\varphi_R(\beta)}{\partial\beta}|H_R(\beta)|^2\right\rangle
\end{aligned} \tag{21}
$$

where we observe that the imaginary part of this expression is equal to the average of the time-delay weighted by the reflectivity. The ensemble average in (21) is calculated as

$$\left\langle \frac{\partial H_R(\beta)}{\partial \beta} H_R^*(\beta) \right\rangle$$
$$= \overline{F}\left(\beta; \left(\frac{\partial \tilde{q}_o(z, \beta)}{\partial \beta} - 2jz\tilde{q}_o(z, \beta) \right), \tilde{q}_o(z, \beta); \gamma \right). \quad (22)$$

From (20)–(22) we estimate the ensemble average of the time-delay as

$$\langle t_d(\beta) \rangle \approx -\frac{n_o}{c} \frac{\left\langle \frac{\partial \varphi_R(\beta)}{\partial \beta} |H_R(\beta)|^2 \right\rangle}{\left\langle |H_R(\beta)|^2 \right\rangle}$$
$$= -\frac{n_o}{c} \frac{\mathrm{Im}\left\langle \frac{\partial H_R(\beta)}{\partial \beta} H_R^*(\beta) \right\rangle}{\langle H_R(\beta) H_R^*(\beta) \rangle} \quad (23)$$

where Im stands for imaginary part, and the two ensemble averages have been calculated in (19) and (22). This result is approximate due to the reflectivity weight term that appears in the time-delay average. Expression (23) would be exact in the limit of very weak correlation between the time delay and reflectivity. For small perturbations, the in-band reflectivity of dispersion compensators will be essentially constant and (23) provides a good approximation for the statistics of the time-delay.

2) Fluctuations of Time Delay: Our main interest, however, is to estimate the standard deviation of the time-delay fluctuations. To achieve this objective, we need to evaluate the ensemble average of the square of the time delay $\langle t_d^2(\beta) \rangle$. We proceed as before, starting with the related ensemble average

$$\left\langle \frac{\partial H_R(\beta)}{\partial \beta} \frac{\partial H_R^*(\beta)}{\partial \beta} \right\rangle$$
$$= \left\langle \left(\frac{\partial \varphi_R(\beta)}{\partial \beta} \right)^2 |H_R(\beta)|^2 + \left(\frac{\partial |H_R(\beta)|}{\partial \beta} \right)^2 \right\rangle$$
$$\approx \left\langle \left(\frac{\partial \varphi_R(\beta)}{\partial \beta} \right)^2 |H_R(\beta)|^2 \right\rangle \quad (24)$$

where we have assumed slow variations for the modulus $|H_R(\beta)|$ of the spectral response within the reflection band. The ensemble average (24) is again calculated in terms of $\overline{F}$ (19)

$$\left\langle \frac{\partial H_R(\beta)}{\partial \beta} \frac{\partial H_R^*(\beta)}{\partial \beta} \right\rangle$$
$$= \overline{F}\left(\beta; \left(\frac{\partial \tilde{q}_o(z, \beta)}{\partial \beta} - 2jz\tilde{q}_o(z, \beta) \right) \right.$$

$$\left. \cdot \left(\frac{\partial \tilde{q}_o(z, \beta)}{\partial \beta} - 2jz\tilde{q}_o(z, \beta) \right); \gamma \right). \quad (25)$$

Now we can estimate $\langle t_d^2(\beta) \rangle$ as

$$\langle t_d^2(\beta) \rangle \approx \left(\frac{n_o}{c} \right)^2 \frac{\left\langle \left(\frac{\partial \varphi_R(\beta)}{\partial \beta} \right)^2 |H_R(\beta)|^2 \right\rangle}{\left\langle |H_R(\beta)|^2 \right\rangle} \quad (26)$$

which can be evaluated from (19), (24), and (25). The variance of the time-delay $\sigma_{td}^2(\beta)$ is finally expressed in terms of (23) and (26) as

$$\sigma_{td}^2(\beta) = \langle t_d^2(\beta) \rangle - \langle t_d(\beta) \rangle^2. \quad (27)$$

The time-delay standard deviation $\sigma_{td}(\beta)$ will be used in Section V to discuss the effect of random phase errors on dispersion compensators.

D. Average for the Reflectivity in OFG with Both Amplitude and Phase-Noise

Amplitude noise can also contribute to the deterioration of the background level in the spectral response of apodized gratings. In this section, we extend the analysis to calculate the ensemble average for the reflectivity of a grating subjected to both amplitude and phase-noise. The main assumption of the calculation is that both noise sources are statistically independent.

Following an analysis similar to that developed in Section III-A and taking into account the autocorrelation (6) for the relative amplitude-noise $F_a(z)$, we calculate the ensemble average of the reflectivity as

$$\langle R(\beta) \rangle = \overline{F}\left(\beta; \tilde{q}_o(z, \beta), \tilde{q}_o(z, \beta); \gamma \right) + \int_0^L dz \, |\tilde{q}_o(z, \beta)|^2 \eta. \quad (28)$$

It is shown that the average reflectivity in this case has two terms. The first one is that corresponding to a grating subjected only to phase-noise (19), while the second contribution is the excess background reflectivity due to a random amplitude as will be discussed in Section IV-B.

IV. EFFECT OF RANDOM PHASE AND AMPLITUDE ERRORS IN APODIZED GRATINGS

Apodized gratings exhibit reduced sidelobes in their spectral response, minimizing crosstalk effects between adjacent optical channels [26]. Their use in WDM communication systems results in efficient utilization of the optical bandwidth [27]. In this section, we study the deterioration of apodized OFG performance due to random phase and amplitude errors incurred during the fabrication process. The most important effect is a reduced isolation of the filtered channel due to an enhancement
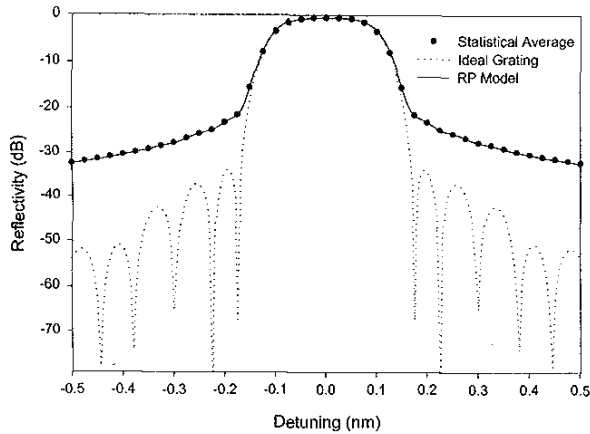
Fig. 2. Reflectivity spectrum of the apodized grating. - - - : Ideal deterministic grating. —: Ensemble average calculated with random phase RP model. •: Values calculated by averaging over 1000 random experiments.
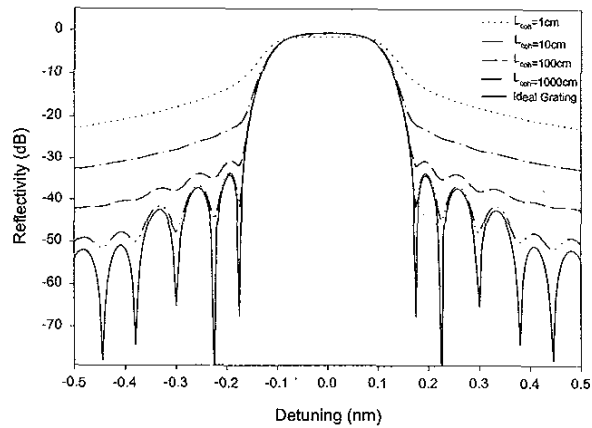

Fig. 3. Ensemble average for the reflectivity spectrum of the apodized grating for various values of the coherence length.

of the sidelobes and a decrease in the sharpness of the filter's bandedge transition.

A. Effects of Phase-Noise

To illustrate the analysis introduced in previous sections, we first consider an OFG with a raised cosine apodization profile. The grating has a total length of 1 cm and a maximum coupling constant q_o^{max} of 3.5 cm^{-1}. The maximum reflectivity of the grating is 90%. Fig. 2 shows the response of the deterministic grating $|H_R^o(\beta)|^2$ which exhibits low sidelobes (dashed line). Let us suppose now that the grating was fabricated with a system that had a coherence length L_{coh} of 10 cm. This corresponds to a standard deviation for the random phase variation along a grating period of 3 mrad. By using the random phase (RP) model previously developed (19) we can calculate the ensemble average for the reflectivity (solid line). We clearly observe a substantial increase in the out-of-band background level and a reduced sharpness of the reflection bandgap edge. The predictions of the RP model were corroborated by statistically averaging the spectral response of 1000 gratings with phase errors randomly generated (solid points in Fig. 2). The agreement between both calculations is very good throughout the reflection spectrum. It is important to note that Monte Carlo-type simulations are very expensive from a computational point of view compared to calculations carried out with the proposed RP model.

In a second numerical experiment we allowed the coherence length of the fabrication system L_{coh} to vary from 1 to 1000 cm. This corresponds to standard deviations for the random phase variation along a grating period that vary from 10 to 0.3 mrad. The ensemble averages of the reflectivity for the cases considered are shown in Fig. 3. We observe that the out-of-band background level increases and the bandedge sharpness decreases as the coherence length is reduced.

The RP model is useful to understand these results and to find the relation between the out-of-band background level and the coherence length of the fabrication system. From (18) and (19) we observe that the ensemble average of the reflectivity is equal to the Fourier transform of the product of the autocorrelation
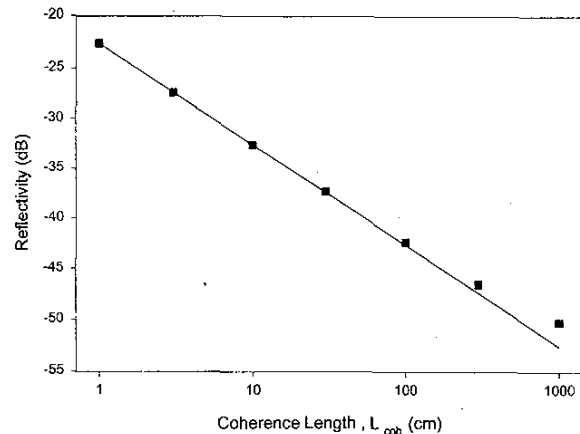
Fig. 4. Ensemble average (•) for the out-of-band reflectivity of the apodized grating at a detuning of 0.5 nm as a function of the coherence length. The solid line (—) is a theoretical fit proportional to L_{coh}^{-1}.

of $\tilde{q}_o(z, \beta)$ with a decaying exponential. This is equivalent to the convolution of the deterministic grating reflectivity with a Lorentzian function that accounts for the reduced coherence of the fabrication system. This spectral response would be identical to that obtained if we analyzed the ideal grating by scanning in wavelength a laser with a finite Lorentzian linewidth. The out-of-band background level is mainly given by the overlap between the reflection band of the grating and the decaying Lorentzian function. A simple integration shows that this overlap is inversely proportional to the coherence length L_{coh}. Fig. 4 shows the out-of-band reflectivity at a detuning of 0.5 nm as a function of the coherence length for the cases previously considered. The solid line is a fit given by

$$\langle R(\beta) \rangle \propto \frac{1}{L_{coh}} \tag{29}$$

that shows the accuracy of the prediction. It can also be shown that the overlap between the reflection band and the Lorentzian
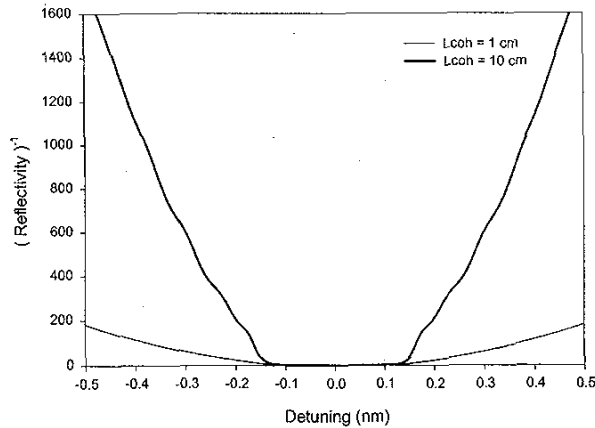
Fig. 5.   Inverse of the reflectivity spectrum of the apodized grating as a function of wavelength detuning for two different coherence lengths, showing an approximate linear relation.
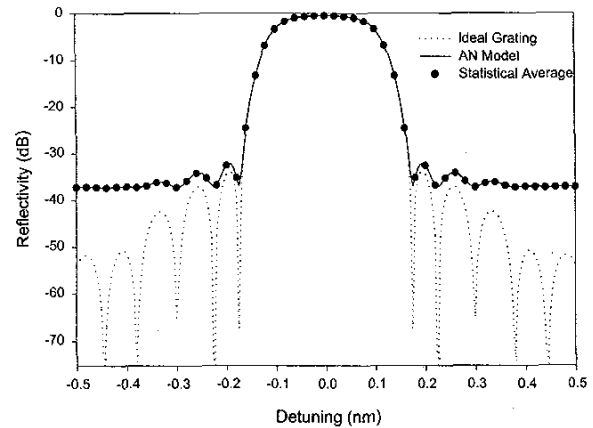

Fig. 6.   Reflectivity spectrum of the apodized grating. - - -: Ideal deterministic grating. ——: Ensemble average calculated with amplitude-noise AN model. •: Values calculated by averaging over 1000 random experiments.

function is approximately inversely proportional to the distance between the detuning β and the band edge β_{EDGE}

$$\langle R(\beta)\rangle \propto \frac{1}{|\beta - \beta_{\mathrm{EDGE}}|}. \tag{30}$$

Fig. 5 illustrates this relation for two different values of the coherence length.

We have shown that the spectral response of apodized gratings is given by the convolution of the ideal deterministic spectral response with a finite linewidth function that accounts for the reduced coherence length of the fabrication system. This translates into a degradation of the spectral isolation of the filter.

B. Effects of Amplitude Noise

We study now the effect of amplitude-noise in the spectral response of apodized gratings. Let us consider again an OFG with a raised-cosine apodization profile, a total length of 1 cm and a maximum coupling constant q_o^{max} of 3.5 cm^{-1}. We assume that the grating is subjected only to an amplitude-noise characterized by an η of $3.9 \cdot 10^{-5}$ cm. According to (7), this means that the standard deviation of the relative amplitude fluctuation is 4.4% if we describe the grating by sampling sections of 200 μm length. Fig. 6 shows the response of the deterministic grating $|H_R^o(\beta)|^2$ and compares it with the ensemble average obtained by means of the amplitude-noise (AN) model developed in Section III. The predictions of this model were again confirmed by statistically averaging the spectral response of 1000 gratings with amplitude-noise randomly generated (solid points in Fig. 6). We observe that the main effect of amplitude noise is a substantial increase of the flat background level of the spectral response.

In a second numerical experiment we allowed the amplitude-noise factor η to vary from $3.9 \cdot 10^{-7}$ to $8 \cdot 10^{-4}$ cm. The ensemble averages of the reflectivity for the cases considered is shown in Fig. 7. In analogy with the phase-noise case, the out-of-band background level increases for higher values of the amplitude-noise factor η.
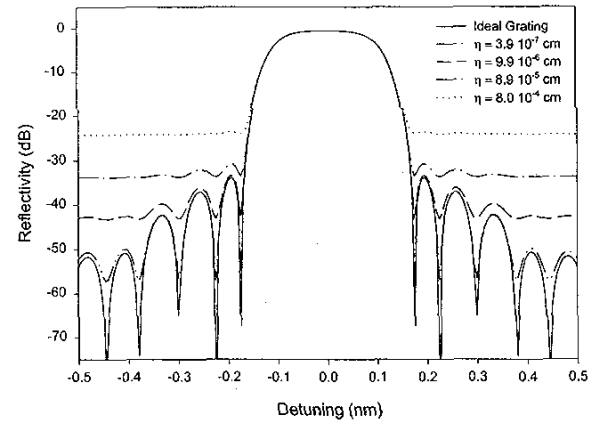
Fig. 7.   Ensemble average for the reflectivity spectrum of the apodized grating for various values of amplitude-noise factor η.

Finally, evaluation of the second term in (28) yields an analytical expression for the excess out-of-band background reflection level, which for gratings with raised-cosine apodization profile is

$$\langle R_{\mathrm{excess}}(\beta_{\mathrm{out-band}})\rangle \approx \int_0^L dz \, |\tilde{q}_o(z, \beta)|^2 \, \eta = \tfrac{3}{8} q_{\mathrm{max}}^2 L\eta. \tag{31}$$

The background level scales with the square of the maximum coupling function q_o^{max}, the length of the grating L, and the noise factor η. Fig. 8 compares the predictions of this analytical formula with the AN model, showing exact agreement for high values of η, where the amplitude-noise dominates the out-of-band reflection.

V. Effects of Random Phase Errors on Chirped Gratings

The main application of chirped OFG is its use for compensation of the second order dispersion in optical communication links [28], [29]. For this purpose, it is important that the time-delay response of the grating exhibits good linearity
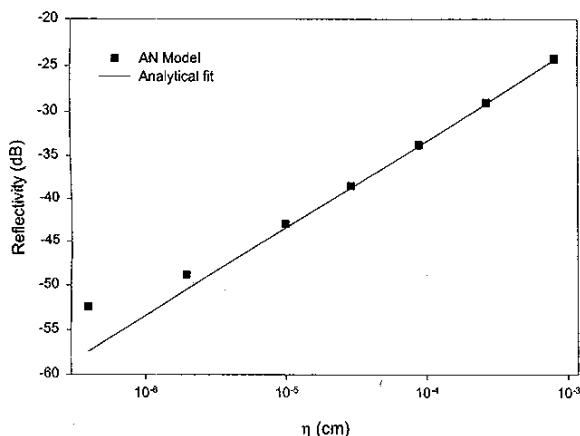
Fig. 8. Ensemble average (■) for the out-of-band reflectivity of the apodized grating at a detuning of 0.5 nm as a function of the amplitude-noise factor η. The solid line (—) is the theoretical fit (31).

to minimize the bit error rate. It has been established that the time-delay linearity improves in nonuniform apodized chirped gratings [25]. In this section we are going to study the effect that a limited coherence length of the fabrication system has on the time-delay linearity of chirped gratings. We will show that the standard deviation of the time-delay fluctuations increases as the coherence length L_{coh} is reduced.

As in the previous section, we illustrate the effects of random phase errors with a practical chirped grating. The grating, described in Fig. 9, has a total length of 15 cm and a raised cosine apodization profile that extends over 2 cm at both ends of the grating. The maximum of the coupling function q_o^{max} is 1.3 cm^{-1} and its deterministic phase $\theta(z)$ was linearly chirped with a chirp-parameter α of 4.92 cm^{-2}

$$\frac{\partial^2\theta(z)}{\partial z^2} = \alpha. \qquad (32)$$

The deterministic spectral response of the grating is shown in Fig. 10. The in-band reflectivity was 90% and the time-delay exhibited good linearity. The grating was designed to compensate a 100-km fiber-link at a wavelength of 1.5 μm for an optical bandwidth of 0.6 nm.

Let us assume now that the grating is fabricated with a system of limited coherence length. By using the random phase model previously developed, we have calculated the standard deviation of the time-delay $\sigma_{td}(\beta)$ for different coherence lengths L_{coh} ranging from 10 to 1000 cm. The results predicted by the model are shown in Fig. 11 by thick solid lines and clearly demonstrate that the time-delay fluctuations increase as the coherence length is reduced. We corroborated these results by statistically averaging the time-delay responses of 50 gratings with randomly generated phase errors distributions (thin lines). The agreement is very good despite the approximations involved in the RP model calculations.

It is also interesting to observe in Fig. 11 that the time-delay fluctuations grow for optical wavelengths that are preferentially reflected toward the end of the grating (negative detunings). As
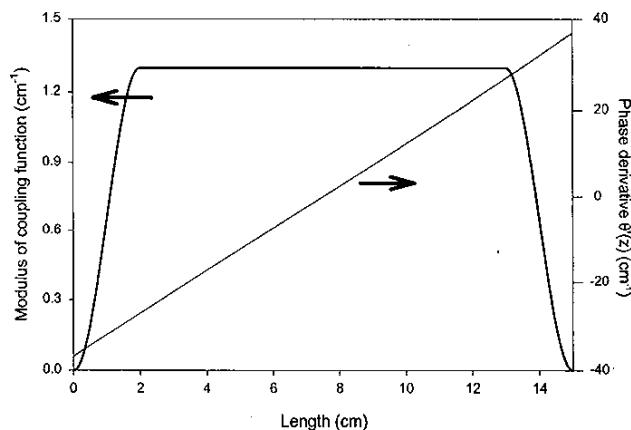
Fig. 9. Modulus and phase derivative of the deterministic coupling function $q_o(z)$ for an apodized chirped grating.
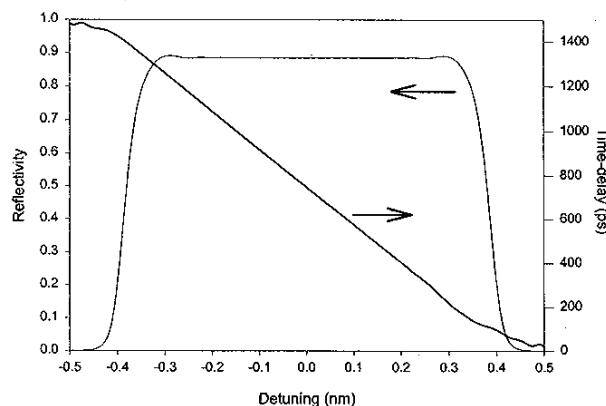
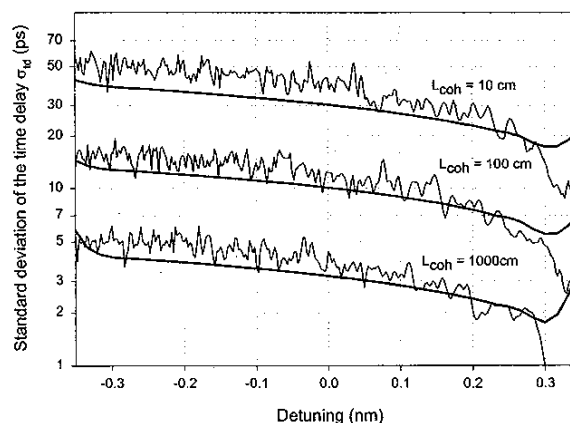Fig. 10. Reflectivity and time-delay response for the chirped grating represented in Fig. 9.

Fig. 11. Spectral evolution for the standard deviation of the time-delay $\sigma_{td}(\beta)$ for different coherence lengths L_{coh}. The thick lines are the results predicted by the RP model, while the thin lines are statistical averages of 50 randomly generated chirped gratings.

these wavelengths are able to penetrate further into the grating, they are also more exposed to the random medium and, consequently, the fluctuations of the time-delay are also higher. This is also the reason why the RP model underestimates slightly the
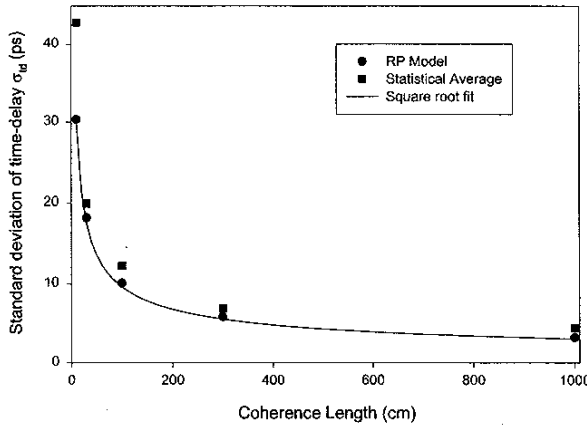
Fig. 14. Standard deviation of the time-delay fluctuations $\sigma_{td}(\beta)$ for three different coupling strengths q_o^{max}: 0.8, 1.3, and 1.9 cm^{-1}. (a) was calculated with the RP model, while (b) shows the average over 50 randomly generated chirped gratings.
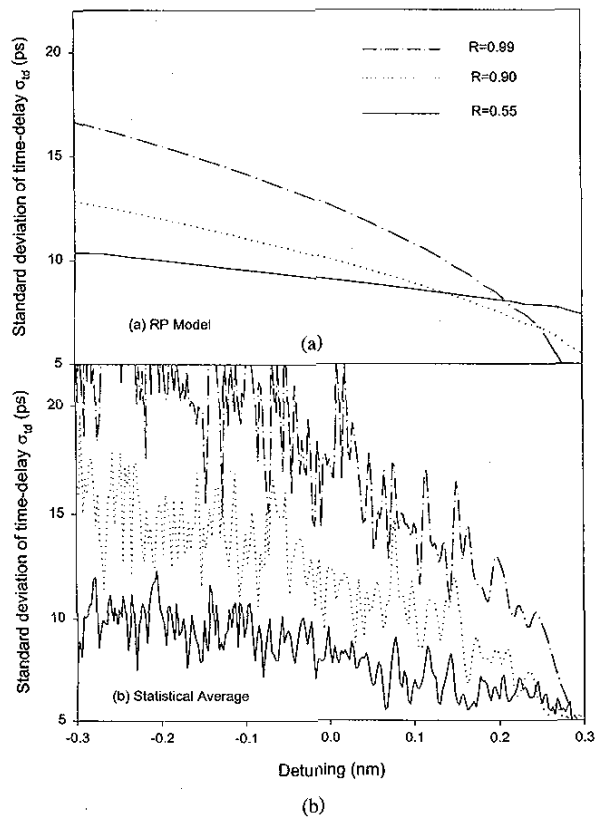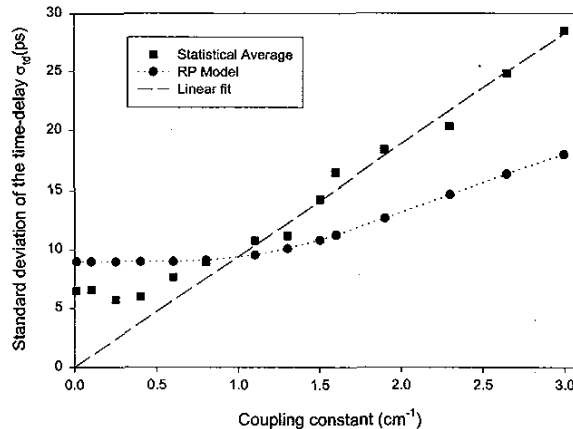

Fig. 15. Standard deviation of the time-delay fluctuations σ_{td} at the center of the reflection band for several coupling strengths q_o^{max}. Points (•) were calculated with the RP model; (■) were calculated averaging over 50 randomly generated chirped gratings; the dashed line (- - -) is a linear fit. The coherence length L_{coh} was kept constant to 100 cm and the chirp-parameter α was 4.92 cm^{-2}.

B. Coupling Strength Dependence

Finally, we are interested in determining the influence of the grating coupling strength on the time-delay fluctuations. We initially considered three cases with maximum coupling function q_o^{max} equal to 0.8, 1.3, and 1.9 cm^{-1}, that corresponded to in-band reflectivities of 50, 90, and 99%. The coherence length of the grating was kept constant at a value of 100 cm. In Fig. 14, we show the standard deviation of the time-delay fluctuations calculated both with the RP model in part (a), and averaging over 50 randomly generated gratings in part (b). We observe good qualitative agreement between both calculations, although the RP model tends to underestimate the standard deviation of the time-delay. The fluctuations of the time-delay clearly increase as the grating coupling strength is higher. Also, the slope for the growth of the fluctuations along the band is larger in this case.

The reason for this behavior can be explained by the fact that strong gratings relax the phase-matching condition in (33) due to their broad bandgap

$$\left| \int_z^{z+\Delta} \frac{\partial \theta(z)}{\partial z} \, dz + (\phi(z + \Delta) - \phi(z)) - 2\beta\Delta \right|$$
$$\leq 2 |q_0^{max}| \, \Delta. \quad (38)$$

Consequently, light of a particular wavelength (or detuning β) can interact efficiently with a larger section of the grating if the coupling strength is high. The size of this region is approximately equal to $4q_o^{max}/\alpha$, increasing linearly with the coupling strength. However, in an ideal noiseless grating the light does not penetrate deep into this region, and is mainly reflected from an initial section of length $1/q_o^{max}$. If the grating is subjected to random phase errors, the light will be allowed to penetrate further into this region of strong interaction and the uncertainty of the reflection point will also be higher. This translates into larger fluctuations of the time-delay, which scale linearly with the size of the interaction region and, consequently, with Fig. 15 shows the linear relationship between q_o^{max} and the standard deviation of the time-delay σ_{td} (at the center of the reflection band) for a constant coherence length of 100 cm. The points in this figure were calculated both with the random phase model (RP) and by statistically averaging the time-delay responses of 50 gratings with randomly generated phase error distributions. The dashed line is a linear fit. For low values of the coupling constant q_o^{max}, the time-delay fluctuation tends to a constant minimum value. Both curves evolve asymptotically toward a linear dependence of σ_{td} with respect to q_o^{max} at high values of the coupling constant. The RP model provides a good approximation for moderate values of q_o^{max} (less than 2 cm^{-1}, that correspond to gratings of reflectivity inferior to 99%), underestimating the time-delay fluctuation at high values of the coupling constant.

As a summary, we have shown that random phase errors give rise to enhanced fluctuations in the time-delay of apodized chirped gratings, degrading their performance as dispersion compensators. We have demonstrated that the standard deviation of the time-delay σ_{td} scales inversely proportional to the chirp-parameter α and also to the square root of the coherence length L_{coh}. Also, the fluctuations of the time-delay are more noticeable for gratings with high reflectivity, scaling linearly with the coupling constant of the grating.

VI. CONCLUSION

In this paper, we have studied the effects of random phase and amplitude errors in the performance of optical filters based on fiber Bragg gratings. The amount of random phase errors introduced in the grating during the writing process can be regarded a measure of the quality of the fabrication system. We have shown that this amount of random phase errors can be quantified through the concept of coherence length, which is applied for first time in this context. A statistical model was developed to calculate the ensemble averages of the main grating spectral parameters in terms of this coherence length. Two particular types of gratings of particular importance for optical communications were analyzed: apodized gratings commonly used in WDM systems, and chirped gratings employed to compensate the fiber dispersion.

The main effects of random phase errors in apodized gratings were an increase in the out-of-band background reflectivity and a reduction in the sharpness of the bandedge as the coherence length is decreased. The background reflectivity scaled inversely proportional to the grating coherence length, and decreased for detunings far away of the bandgap edge. Amplitude errors also gave rise to an increase in the out-of-band background reflectivity. In this case, however, the background level remained constant as a function of detuning. The method presented permits the calculation of the minimum coherence length L_{coh} and maximum amplitude noise factor η that can be allowed to achieve a required crosstalk level between different WDM channels.

In the case of apodized chirped gratings, the random phase errors gave rise to enhanced fluctuations of the time-delay spectral response, degrading their performance as dispersion compensators. The standard deviation of the time-delay scaled inversely proportional to the chirp-parameter and also to the square root of the coherence length. Also, the fluctuations of the time-delay were larger for gratings of higher reflectivity. Grating fabrication systems with long coherence lengths are necessary to minimize these negative effects.

REFERENCES

[1] B. Crosignani, P. Di Porto, and M. Bertolotti, *Statistical Properties of Scattered Light*, New York: Academic, 1975.

[2] E. Brinkmeyer, "Analysis of the backscattering method for single-mode optical fibers," *J. Opt. Soc. Amer.*, vol. 70, no. 8, pp. 1010–1012, Aug. 1980.

[3] A. Basu and J. M. Ballantyne, "Random fluctuations in first-order waveguide grating filters," *Appl. Opt.*, vol. 18, no. 15, pp. 2575–2579, Aug. 1979.

[4] H. E. Rowe, "Propagation in one-dimensional random media," *IEEE Trans. Microwave Theory Tech.*, vol. 19, pp. 73–79, Jan. 1971.

[5] D. Marcuse, "Coupled power equations for backward waves," *IEEE Trans. Microwave Theory Tech.*, vol. 20, pp. 541–546, Aug. 1972.

[6] J. McKenna and J. A. Morrison, "Moments and correlation functions of solutions of a stochastic differential equation," *J. Math. Phys.*, vol. 11, no. 8, pp. 2348–2360, Aug. 1970.

[7] R. Adar, C. H. Henry, M. A. Milbrodt, and R. C. Kistler, "Phase coherence of optical waveguides," *J. Lightwave Technol.*, vol. 12, pp. 603–606, Apr. 1994.

[8] C. Dragone, "Cross-talk caused by fabrication errors in a generalized Mach–Zehnder interferometer," *Electron. Lett.*, vol. 33, no. 15, pp. 1326–1327, July 1997.

[9] G. Meltz, W. W. Morey, and W. H. Glen, "Formation of Bragg gratings in optical fibers by a transverse holographic method," *Opt. Lett.*, vol. 14, no. 15, pp. 823–825, Aug. 1989.

[10] W. H. Loh, M. J. Cole, M. N. Zervas, S. Barcelos, and R. I. Laming, "Complex grating structures with uniform phase masks based on the moving fiber-scanning technique," *Opt. Lett.*, vol. 20, no. 20, pp. 2051–2053, Oct. 1995.

[11] A. Asseh, H. Storoy, B. E. Sahlgren, S. Sandgren, and R. A. H. Stubbe, "A writing technique for long fiber Bragg gratings with complex reflectivity profiles," *J. Lightwave Technol.*, vol. 15, pp. 1419–1423, Aug. 1997.

[12] F. Ouellette, "The effect of profile noise on the spectral response of fiber gratings," in *Bragg Gratings, Photosensitivity and Poling in Glass Fibers and Waveguides: Applications and Fundamentals*. Williamsburg, VA: BMG, Oct. 1997, vol. 13-1, pp. 222–224.

[13] K. O. Hill, B. Malo, F. Bilodeau, D. C. Johnson, and J. Albert, "Bragg gratings fabricated in monomode photosensitive optical fiber by UV exposure through a phase mask," *Appl. Phys. Lett.*, vol. 63, no. 10, pp. 1035–1037, Mar. 1993.

[14] D. Z. Anderson, V. Mizrahi, T. Erdogan, and A. E. White, "Production of in-fiber gratings using a diffractive optical element," *Electron. Lett.*, vol. 29, no. 6, pp. 566–568, Mar. 1993.

[15] B. Malo, K. O. Hill, F. Bilodeau, D. C. Johnson, and J. Albert, "Point-by-point fabrication of micro-Bragg gratings in photosensitive fiber using single excimer pulse refractive index modification techniques," *Electron. Lett.*, vol. 29, no. 18, pp. 1668–1669, Sept. 1993.

[16] J. Martin and F. Ouellette, "Novel writing technique of long and highly reflective in-fiber gratings," *Electron. Lett.*, vol. 30, no. 10, pp. 811–812, May 1994.

[17] M. Ibsen, M. K. Durkin, M. J. Cole, and R. I. Laming, "Optimized square passband fiber Bragg grating filter with in-band flat group delay response," *Electron. Lett.*, vol. 34, no. 8, pp. 800–801, Apr. 1998.

[18] J. Skaar, B. Sahlgren, P. Y. Fonjallaz, H. Storoy, and R. Stubbe, "High-reflectivity fiber-optic bandpass filter designed by use of the iterative solution to the Gel'fan-Levitan-Marchenko equations," *Opt. Lett.*, vol. 23, no. 12, pp. 933–935, June 1998.

[19] A. Papoulis, *Probability, Random Variables and Stochastic Processes*, 3rd ed. New York: McGraw-Hill, 1999.

[20] B. Oksendal, *Stochastic Differential Equations*, 5th ed, New York: Springer, 1998, ch. 2.

[21] C. H. Henry, "Theory of the linewidth of semiconductor lasers," *IEEE J. Quantum Electron.*, vol. 18, no. 2, pp. 259–264, Feb. 1982.

[22] H. Kogelnik and C. V. Shank, "Coupled-wave theory of distributed feedback lasers," *J. Appl. Phys.*, vol. 43, no. 5, pp. 2327–2335, May 1972.

[23] A. Yariv, "Coupled-mode theory for guided-wave optics," *IEEE J. Quantum Electron.*, vol. 9, pp. 919–933, Sept. 1973.

[24] T. Erdogan, "Fiber grating spectra," *J. Lightwave Technol.*, vol. 15, pp. 1277–1294, Aug. 1997.

[25] K. Ennser, M. N. Zervas, and R. I. Laming, "Optimization of apodized linearly chirped fiber gratings for optical communications," *IEEE J. Quantum Electron.*, vol. 34, pp. 770–778, May 1998.

[26] H. Kogelnik, "Filter response of nonuniform almost-periodic structures," *Bell Syst. Tech. J.*, vol. 55, no. 1, pp. 109–126, Jan. 1976.

[27] T. A. Strasser, P. J. Chandonnet, J. DeMarco, C. E. Soccolich, J. R. Pedrazzani, D. J. DiGiovanni, M. J. Andrejco, and D. S. Shenk, "UV-induced fiber grating OADM devices for efficient bandwidth utilization," in *Proc. Opt. Fiber Commun. (OFC) Conf.*, 1996, pp. PD8.1–PD8.5.

[28] F. Ouellette, "Dispersion cancellation using linearly chirped grating filters in optical waveguides," *Opt. Lett.*, vol. 12, no. 10, pp. 847–849, Oct. 1987.

[29] M. J. Cole, H. Geiger, R. I. Laming, S. Y. Set, M. N. Zervas, W. H. Loh, and V. Gusmeroli, "Broadband dispersion-compensating chirped fiber Bragg gratings in a 10 Gbit/s NRZ 110 km nondispersion-shifted fiber link operating at 1.55 μm," *Electron. Lett.*, vol. 33, no. 1, pp. 70–71, Jan. 1997.

Ricardo Feced received the Telecommunications Engineering degree from Madrid Polytechnic University, Spain, in 1993 and the Ph.D. degree in electronic engineering from King's College London, U.K., in 1998.

He has been with the ORC, Southampton, U.K., as a Research Fellow since the beginning of 1998. His research interests include fiber grating devices, DFB lasers, and nonlinear optics.

Mikhail N. Zervas was born in Dimaina-Nafplias, Greece, in 1959. He received the Diploma degree in electrical engineering from Aristotle University of Thessaloniki, Greece, in 1983, the M.Sc. degree in applied and modern optics from the University of Reading, U.K., in 1985 (with distinction), and the Ph.D. degree in fiber optics from the University College London, U.K., in 1989.

During his postgraduate studies, he was awarded scholarships from the State Scholarships Foundation of Greece (IKY) and the Bodassakis Foundation, Athens, Greece. In 1990, he was appointed Lecturer in the Faculty of Electrical Engineering, University of Thessaloniki. In 1991, he joined the Optoelectronics Research Center, University of Southampton as a Research Fellow. In 1995, he was promoted full Professor at the Optoelectronics Research Center, and Electronics and Computer Science Department of the University of Southampton. His main research interests are in the areas of erbium-doped fiber amplifiers, dispersion compensation, fiber gratings, surface-plasmon-polaritons and distributed feedback fiber lasers. He is the author and coauthor of more than 100 technical publications and ten patents. He has served as a member of program committees of various international conferences.

Dr. Zervas was the general Co-Chair at the 1999 Optical Amplifiers Meeting and Their Applications. In 1996, he shared a prize on "metrology for world class manufacturing awards" for his contribution on the development of a high-accuracy fiber grating characterization system.